Effects of Geometric Parameters on the Pin-bearing Strength of Glass/Polyphenylenesulphide Composites

TANER YILMAZ* AND TAMER SINMAZCELIK
Kocaeli University, Mechanical Engineering Department
Engineering Faculty, Veziroglu Campus, Izmit, 41040, Turkey

ABSTRACT: In this experimental study, under conditions of static loading, load-bearing performance of pin connected multilayered (angle-ply) glass fiber-reinforced polyphenylenesulphide matrix composites with $[(0^\circ/90^\circ)]_{4s}$ and $[(0^\circ/90^\circ)/(+/-45^\circ)]_{2s}$ stacking sequence was analyzed. The experiments were carried out according to the ASTM D953. The ratio of the distance between pin center and sample end, to pin diameter E/D; and the ratio of sample width to pin diameter W/D, were changed systematically during the experiments. From the results of the experiment, maximum bearing failure loads were obtained for $[(0^\circ/90^\circ)/(+/-45^\circ)]_{2s}$ lay-up with geometric parameters of $D = 10$ mm and $W/D = 2$. Macro images belonging to failure modes, which occurred as results of the tests were examined. In addition to this, from the fractographic examinations carried out with scanning electron microscope, it was concluded that the geometric parameters intimately affect fracture morphology.

KEY WORDS: bearing, glass fibers, lay-up, pin-loaded joints, SEM.

INTRODUCTION

COMPOSITE MATERIALS ARE widely used in airplane, marine, automotive, and military applications. In these applications, one of the popular methods used to connect two or more components is pin joints. In order to achieve such a connection, it is necessary that firstly holes should be machined on the composite plaques to be connected. In structural elements composed of composite layers (like in airfoils), the holes may cause changes in structural character. In such composite structures, stress concentrations form around the hole and these concentrations decrease the strength and fatigue life of the structure. So, in order that the structure which will be obtained by means of assembling composite

*Author to whom correspondence should be addressed. E-mail: taneryilmaz2002@yahoo.com
Figures 2, 14 and 15 appear in color online: http://jcm.sagepub.com

0021-9983/09/20 2239–15 $10.00/0 DOI: 10.1177/0021998309344455

materials with mechanically fastened connections be safe, the behaviors of materials under loading are necessary to be known.

This topic has attracted attention of many researchers [1–14]. They have shown that for a fixed laminate, the actual failure mode occurring in a bolted or pinned joint is mainly affected by geometric parameters, such as side distance, end distance, hole diameter, hole arrangement, and spacing. Unfortunately, the values of the previous factors to be assumed in order to prevent sudden structural collapse are dependent on the material concerned, so that at this time large experimental databases are required to guarantee safe joint design.

In this study, failure loads and modes, of multilayered glass fiber-reinforced PPS matrix composites with $[(0^\circ/90^\circ)]_{4s}$ and $[(0^\circ/90^\circ)/(+/-45^\circ)]_{2s}$ stacking sequence, developing depending on E/D and W/D ratios as a result of loading with pin were experimentally examined. It is very important to fundamentally characterize the damage mechanisms of pinned composite joints as a function of geometry and ply orientation. An optimal design in composite structures can be achieved by understanding the failure mechanisms in composite laminates. Composite laminates with same E/D and W/D ratios but different stacking sequences have different bearing failure load values and failure modes [15–18]. Therefore, the tests were carried out in order to determine the effect of fiber orientation on failure strength and failure mode. In the study, the aim was determining the maximum load to be applied for each geometric parameter that will not cause any failure in the connection area and the failure mode that will form. Hence, the geometric parameters were varied systematically during the experiments. The knowledge of the failure mode and failure strength would give a chance to select the optimum joint size.

EXPERIMENTAL METHOD AND MATERIALS

In the study, composite plaques connected with a pin having a circular hole were used. Strength of the pin used in the connection is much higher than the strength of composite plaque, thus the pin deformation was neglected. Polished pin made of Ck 45 steel was mounted through the hole in the composite sample without clearance. Sample geometry and pin tensile test device are shown in Figure 1. There is a hole with D diameter, which is located on the symmetry axis at a distance of E from the end of test sample. The uniform tensile load F, applied to the sample is transferred to the composite laminate by means of the pin; the pin is also fixed with a device from outside. The F load applied is symmetrical and parallel with respect to the sample axis. The samples were cut out of the 2 mm thick laminates using a diamond-coated wheel saw. In order to minimize the effects of delamination from drill breakout the specimens were drilled with high steel speed (HSS) drill, which had three welded carbide tips.

The composites used in this study were provided from Ten Cate (Nijverdal/The Netherlands) Company in the form of $450 \times 450 \times 2\,\text{mm}^3$ dimensioned hot pressed laminates. Glass/PPS composite laminates with $[(0^\circ/90^\circ)]_{4s}$ and $[(0^\circ/90^\circ)/(+/-45^\circ)]_{2s}$ stacking sequence contain fiber with a volume of 48%. Composite laminates comprise a total of eight layers. Unit layer thickness and unit layer weight are 0.25 mm and $475\,\text{g/m}^2$, respectively. Mercantile code of composite laminates is GF0303.

Samples to be tested were prepared according to the geometric parameters given below. Keeping W/D ratio constant as 2, 4, and 8, E/D ratios were changed to be 1, 2, 4, and 6 (Table 1).

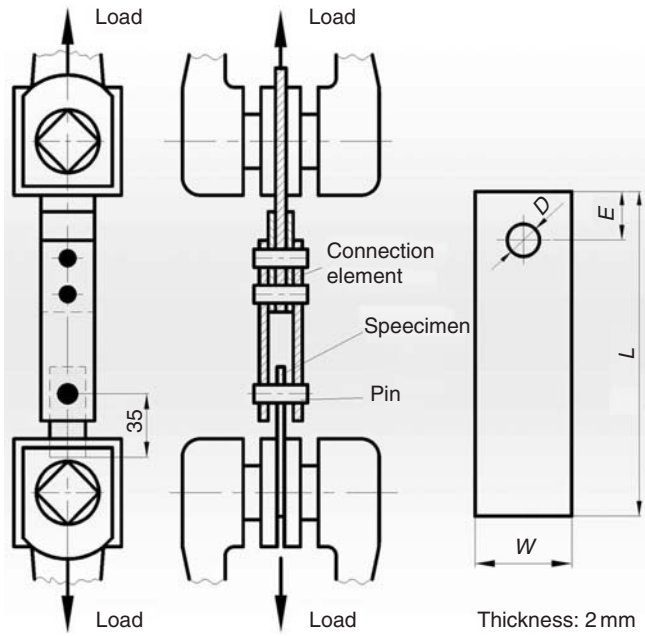

Figure 1. *Test fixture and geometric parameters of tested samples.*

Table 1. Geometry of the joints and pins.

L (mm)	*W* (mm)	*D* (mm)	*W*/*D*	*E*/*D*
40, 45, 55, 65, 75, 95	20, 40	5, 10	2, 4, 8	1, 2, 4, 6

We observed the fracture surfaces from the test samples under a scanning electron microscope (SEM) (JEOL/EO JSM-6060).

Distance from the hole center to the clamped edge and the sample thickness are kept as constants (35 and 2 mm, respectively). The tests were carried out in an Instron 1411 testing machine at a cross-head speed of 1 mm/min. The tensile tests were performed according to ASTM D 953-D standard test method [19]. The samples were tested by means of the pin and a device made of steel. There is a clearance between the device and sample surfaces. During the time from the beginning of loading to fracture development, the way that sample geometry, pin diameter, hole position and especially sample width affected failure mode was observed. Load–displacement curves were drawn for different composite lay-ups and failure modes. For each geometric parameter, a minimum of eight samples were tested and in the calculations the average of these values were used.

RESULTS AND DISCUSSION

In this study, for different geometric parameters, three basic failure modes (bearing, shear out, and net tension) were compared. Typical load–displacement curve obtained from the experiments is shown in Figure 2. The curve displays linear increase until its

maximum value. After that value, deviation from the linear increase and decrease in the load occurs and that is caused by delaminations, matrix cracks, fiber buckling, and breakage. Bearing failure is the safest mode; the material continues carrying load until the last fracture develops. A connection type having damage tolerance before fracture is in question. The bearing mode of failure occurring with the effect of pin loading is in the form of the pin crushing the plaque.

Net tension failure occurs when the cross-section area is minimum. That kind of failure is frequently seen in the condition that sample width W is small and end distance from the hole center is large. When the sample width is increased but the end distance from the hole center is kept small, shear out failure develops. In conditions where the end distance E is short, failure spreads quickly.

Load values for glass/PPS composite materials with $[(0^\circ/90^\circ)]_{4s}$ and $[(0^\circ/90^\circ)/(+/-45^\circ)]_{2s}$ layups, and different W/D and E/D ratios are given in Figures 3 and 4. In order to obtain the

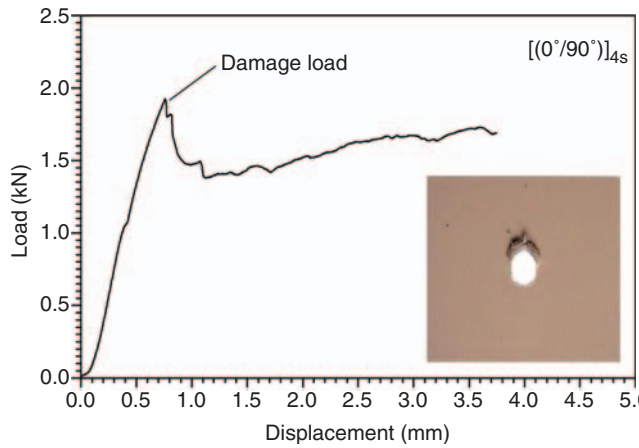

Figure 2. *Typical load–displacement curve with photograph.*

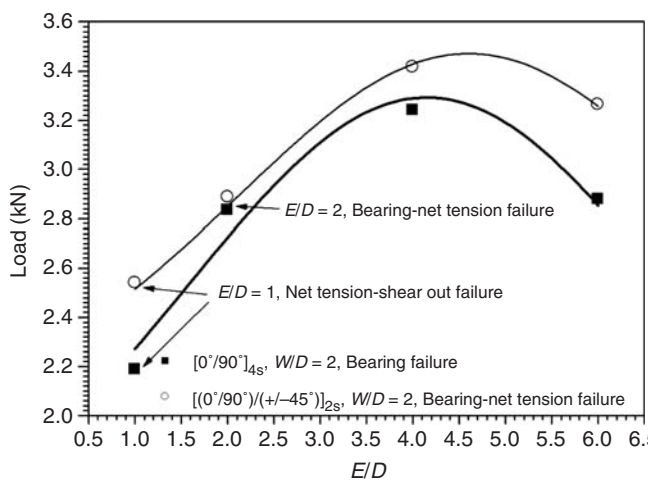

Figure 3. *Ultimate loads of $[(0^\circ/90^\circ)]_{4s}$ and $[(0^\circ/90^\circ)/(+/-45^\circ)]_{2s}$ laminates (W/D = 2, D = 10 mm).*

optimum geometric parameters for these configurations, the ratio of the distance between pin center and the sample end to pin diameter E/D, and the ratio of sample width to pin diameter W/D were systematically changed during the tests. As seen in both of the figures, ultimate load values of laminates with $[(0^\circ/90^\circ)/(+/-45^\circ)]_{2s}$ stacking sequence is higher than the $[(0^\circ/90^\circ)]_{4s}$ joints. In both stacking sequences, maximum load value was obtained when $E/D=4$. In both stacking sequences, when $E/D=1$ and $W/D=2$ mixed failure mode (net tension and shear out) occurred. In $[(0^\circ/90^\circ)]_{4s}$ joints, when $E/D=2$ and $W/D=2$, bearing and net tension failure mode developed (Figure 3). In $[(0^\circ/90^\circ)/(+/-45^\circ)]_{2s}$ joints, when $E/D=1$ and $W/D=4$ bearing and net tension failure modes; in $[(0^\circ/90^\circ)]_{4s}$ stacking sequence when $E/D=1$ and $W/D=4$ shear out failure mode developed (Figure 4).

In Figure 5, ultimate load values developing according to the E/D ratio in $[(0^\circ/90^\circ)/(+/-45^\circ)]_{2s}$ joints are seen. In these joints, if $D=5$ mm for each E/D ratio, bearing failure

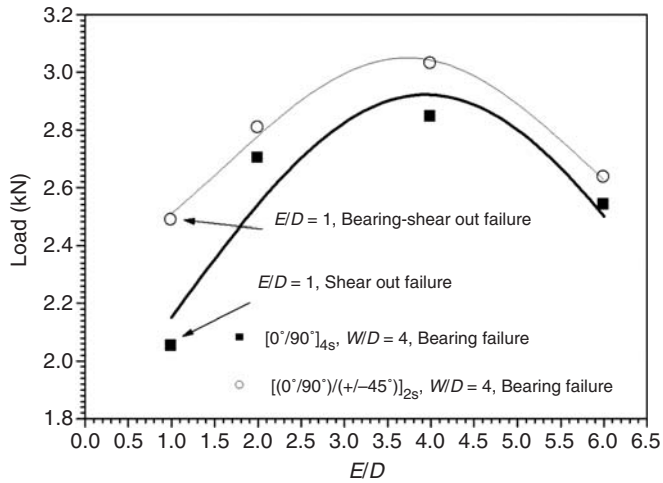

Figure 4. *Ultimate loads of $[(0^\circ/90^\circ)]_{4s}$ and $[(0^\circ/90^\circ)/(+/-45^\circ)]_{2s}$ laminates (W/D = 4, D = 10 mm).*

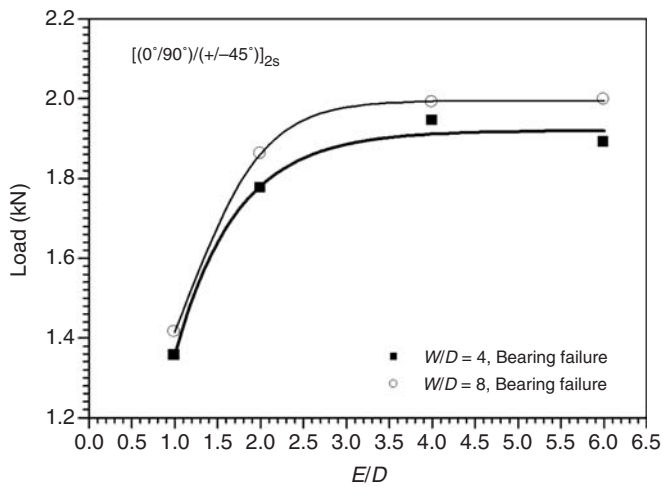

Figure 5. *Ultimate loads of $[(0^\circ/90^\circ)/(+/-45^\circ)]_{2s}$ laminates (D = 5 mm).*

mode developed. As seen in the figure, maximum ultimate load value was obtained when E/D ratio is equal to 4. After that value, any distinct change did not occur. Thus, depending on that result, the critical E/D value was 4. In Figure 6, ultimate load values according to the W/D ratio in $[(0^\circ/90^\circ)/(+/-45^\circ)]_{2s}$ joints are given. The most important point expressed this way is that, when $D=5$ mm the increase in W/D ratio causes increase in ultimate load values. This situation is valid only for laminates having $[(0^\circ/90^\circ)/(+/-45^\circ)]_{2s}$ stacking sequence and only with geometric parameters given in the figure.

Ultimate load values changing depending on the E/D ratio in composite with $[(0^\circ/90^\circ)]_{4s}$ layup are given in Figure 7. When $E/D=1$, $D=5$ mm, $W/D=4$, and W/D = 8, for both conditions the connection area is subjected to shear out failure mode. Minimum bearing load values were obtained when $E/D=1$. For other E/D ratios bearing failure occurred. In Figure 8, ultimate load values versus W/D ratio were given for $[(0^\circ/90^\circ)]_{4s}$ joints when $D=5$ mm. In this graph, the point that attracts attention is that the increase in W/D ratio

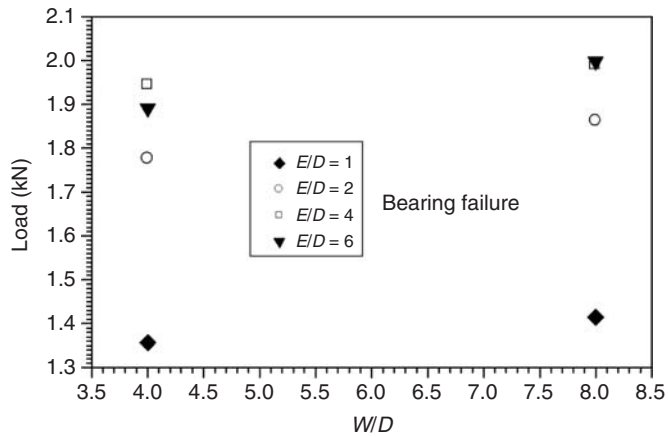

Figure 6. *Ultimate bearing failure loads versus W/D for $[(0^\circ/90^\circ)/(+/-45^\circ)]_{2s}$ joints ($D=5$ mm).*

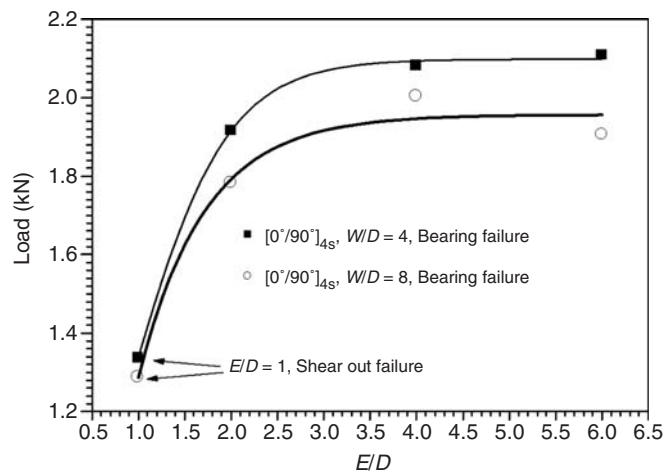

Figure 7. *Ultimate loads of $[(0^\circ/90^\circ)]_{4s}$ laminates ($D=5$ mm).*

causes decrease in ultimate load values. As a result; in the laminate which has $[(0°/90°)/(+/-45°)]_{2s}$ stacking sequence when $D = 5$ mm, the increase in W/D ratio causes increase in ultimate load values; in the composite which has $[(0°/90°)]_{4s}$ stacking sequence when $D = 5$ mm the increase in W/D ratio causes decrease in ultimate load values (Figures 6 and 8).

In Figure 9, for both the $[(0°/90°)]_{4s}$ and $[(0°/90°)/(+/-45°)]_{2s}$ lay-ups, ultimate load values for each parameter that was examined are given. Maximum ultimate load values were obtained for composite laminates with $[(0°/90°)/(+/-45°)]_{2s}$ stacking sequence with $E/D = 4$, $W/D = 2$, and $D = 10$ mm geometric parameters. As seen in Figure 9, minimum bearing failure loads were observed in $[(0°/90°)/(+/-45°)]_{2s}$ lay-up, with $W/D = 4$ and $D = 5$ mm geometry. For both lay-ups when $D = 10$ mm, ultimate load values were greater than $D = 5$ mm. In the condition that the geometric parameters are the same ($D = 10$ mm, $W/D = 2$, $W/D = 4$); $[(0°/90°)/(+/-45°)]_{2s}$ joints display higher resistance than $[(0°/90°)]_{4s}$ joints against loading. But when $D = 5$ mm, $W/D = 4$ and $W/D = 8$, laminates with $[(0°/90°)]_{4s}$ stacking sequence make up more rigid connections with respect to $[(0°/90°)/(+/-45°)]_{2s}$ joints.

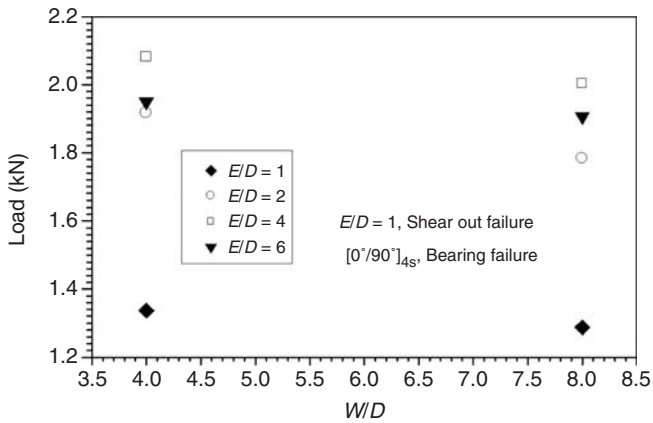

Figure 8. *Ultimate bearing failure loads versus W/D for $[(0°/90°)]_{4s}$ joints ($D = 5$ mm).*

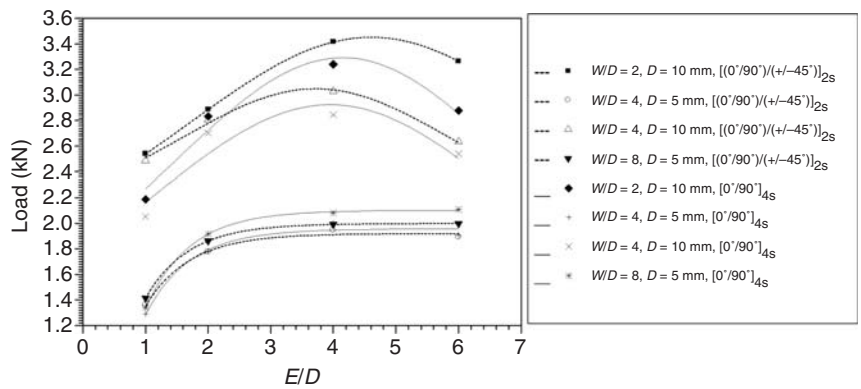

Figure 9. *Ultimate bearing failure loads versus (E/D) for $[(0°/90°)]_{4s}$ and $[(0°/90°)/(+/-45°)]_{2s}$ joints.*

Figure 10 illustrates load–displacement curves of $[(0^\circ/90^\circ)]_{4s}$ joints which have same E/D ratio and W value of 2 and 40 mm, respectively. Slope of the load–displacement curve in the elastic region of a laminate with $W/D = 4$ and pin diameter $D = 10$ mm is higher than the laminate with $W/D = 8$ and pin diameter $D = 5$ mm. When the figure was examined carefully, higher maximum ultimate load values were obtained when $D = 10$ mm rather than $D = 5$ mm. The area below the load–displacement curve gives the energy absorbed by the sample during the test. There is significant difference between the energies absorbed by the tested sample.

Load–displacement curves of the laminate with $[(0^\circ/90^\circ)/(+/-45^\circ)]_{2s}$ stacking sequence and different pin diameters ($D = 5$ mm, 10 mm) are shown in Figure 11. As can be seen from the figure, although the sample width W and E/D ratio are the same, in the samples tested with different pin diameters, different failure modes were encountered. When $D = 5$ mm, shear out failure mode and when $D = 10$ mm, net tension failure mode developed.

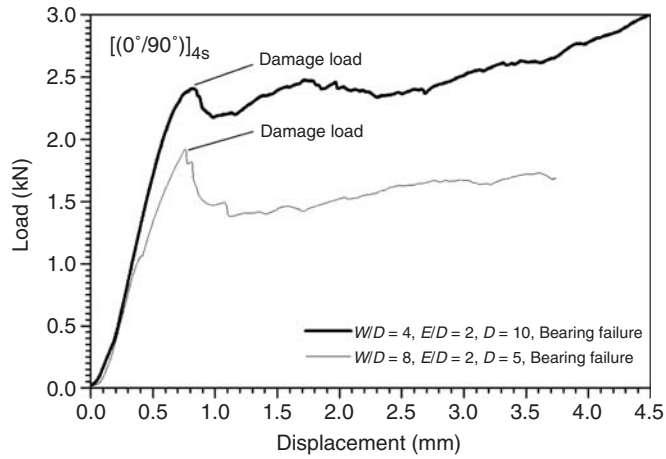

Figure 10. *Load–displacement curves for $[(0^\circ/90^\circ)]_{4s}$ joints ($W = 40$ mm).*

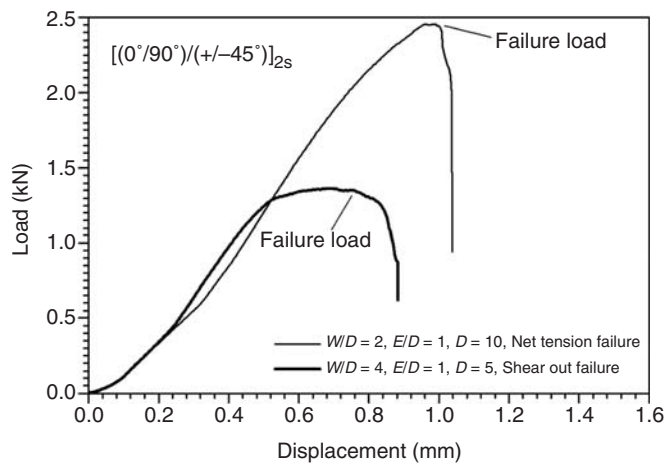

Figure 11. *Load–displacement curves for $[(0^\circ/90^\circ)/(+/-45^\circ)]_{2s}$ joints ($W = 20$ mm).*

The energy amount absorbed by the sample which has net tension failure is greater than the one which has shear out failure. In the beginning, the load–displacement curves increased linearly but after the first failure load, values supported by the samples decreased. When a cross-section area of the sample was small, net tension failure mode development was inevitable. Typical characteristic differences of failure modes appeared after the development of first failure in the load-displacement curve; it was observed that the load values suddenly dropped to zero in net tension and shear out failure modes. Connections facing this mode of failure do not have the tolerance of failure before fracture.

Load–displacement curves of composite laminates with $[(0^\circ/90^\circ)/(+/-45^\circ)]_{2s}$ and $[(0^\circ/90^\circ)]_{4s}$ stacking sequences and same geometric parameters are shown in Figure 12. Slopes belonging to both laminates are very close to each other in the elastic region. Ultimate bearing failure load values of the composite laminate with $[(0^\circ/90^\circ)/(+/-45^\circ)]_{2s}$ stacking sequence is greater than the $[(0^\circ/90^\circ)]_{4s}$ lay-up.

In Figure 13, load–displacement curves of composite laminates with $[(0^\circ/90^\circ)/(+/-45^\circ)]_{2s}$ and $[(0^\circ/90^\circ)]_{4s}$ stacking sequence, and $W/D=2$, $E/D=2$, $D=10\,\text{mm}$

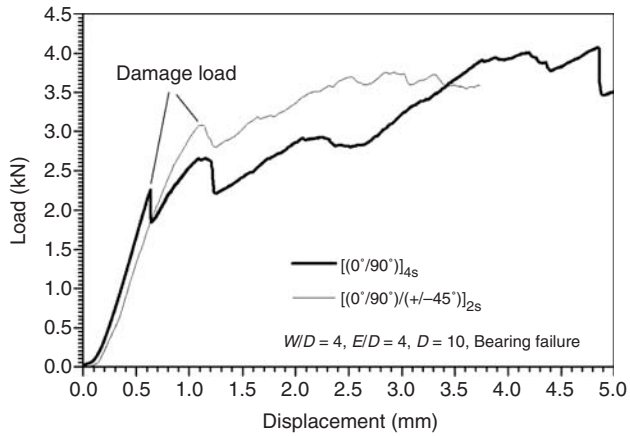

Figure 12. *Load–displacement curves for $[(0^\circ/90^\circ)/(+/-45^\circ)]_{2s}$ and $[(0^\circ/90^\circ)]_{4s}$ joints ($W=40\,\text{mm}$).*

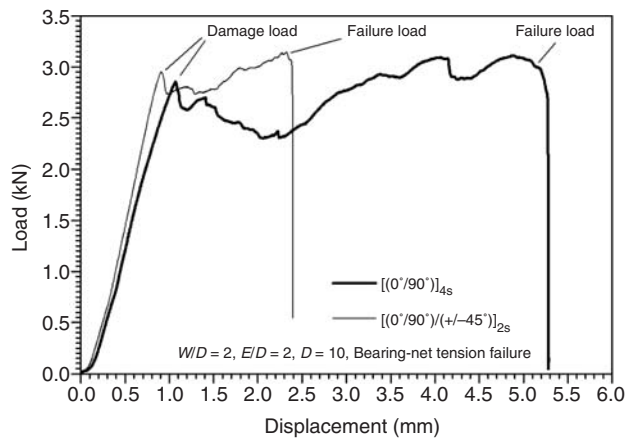

Figure 13. *Load–displacement curves for $[(0^\circ/90^\circ)/(+/-45^\circ)]_{2s}$ and $[(0^\circ/90^\circ)]_{4s}$ joints ($W=20\,\text{mm}$).*

geometric parameters are shown. In $[(0^\circ/90^\circ)/(+/45^\circ)]_{2s}$ joints, the first failure developed at greater load values. For both lay-ups, the slopes in the elastic regions are approximately the same. During test, $[(0^\circ/90^\circ)]_{4s}$ joints absorbed approximately twice the energy than the $[(0^\circ/90^\circ)/(+/-45^\circ)]_{2s}$ joints. For both lay-ups, the load displayed linear increase until the point at which the first failure developed. After that point, the connection area continued to carry the load until it completely failed and with the final fracture a sudden decrease was observed in the load.

In Figures 14 and 15, failures developing in the connection areas of the composite laminates are seen. In the composite with $[(0^\circ/90^\circ)]_{4s}$ stacking sequence given in Figure 14(a), the first bearing failure mode developed and the connection continued to carry the load until a certain value; but when the effect of the load continued, failure was sudden and it developed as fracture. In Figure 14(b) shear out, in 14(c) and (d) bearing failure modes are observed. Bearing-net tension, shear out and bearing failure modes developing in $[(0^\circ/90^\circ)/(+/-45^\circ)]_{2s}$ joints with different geometric parameters are given in Figure 15(a–d), respectively.

In Figure 16(a), failure developed on the net tension plane of a glass/PPS composite with $[(0^\circ/90^\circ)/(+/-45^\circ)]_{2s}$ stacking sequence. In $+45$, -45, and 90 plies, cracks in the matrix developed. Also, in $+45$ and -45 plies; delaminations occurred due to the shear stress developing because of the upward movement of the pin. Delaminations may develop in the

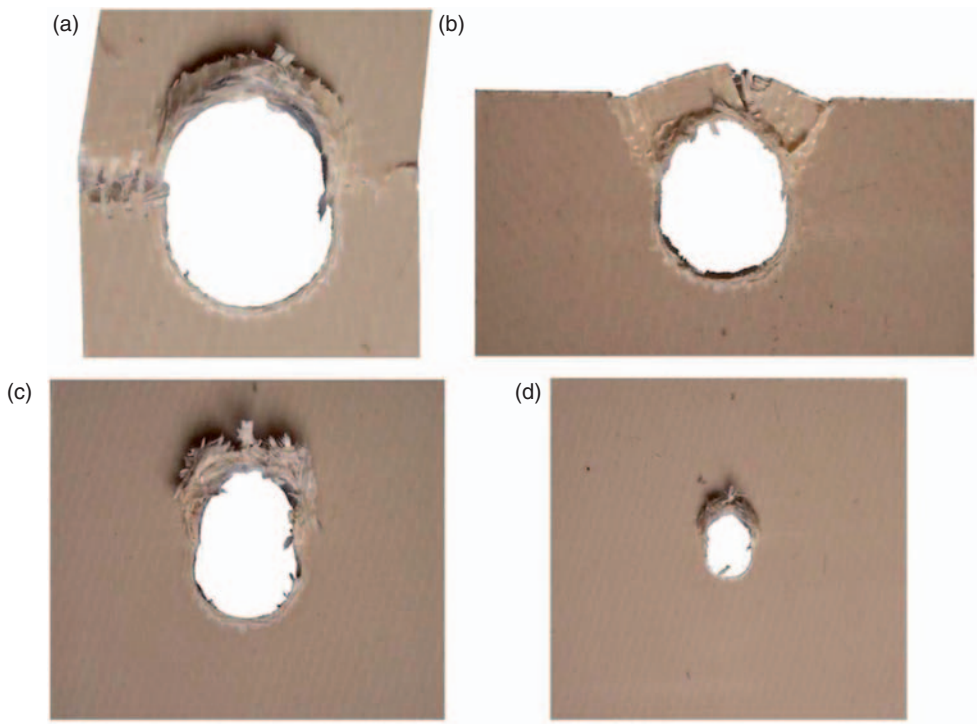

Figure 14. *Photographs of failed pin-loaded $[(0^\circ/90^\circ)]_{4s}$ joints: (a) bearing-tension failure (E/D = 2, W/D = 2, D = 10 mm), (b) shear out failure (E/D = 1, W/D = 4, D = 10 mm), (c) bearing failure (E/D = 2, W/D = 4, D = 10 mm), (d) bearing failure (E/D = 4, W/D = 8, D = 5 mm).*

matrix cracks of these plies. In the 90 ply, there are cracks in the matrix and delaminations in the fiber/matrix interface. Besides, the fractures developing the fibers are clearly seen. In Figure 16(b), fiber breakage, cracks in matrix, and fracture developing in the composite laminate as a result of the propagation of the pin are observed.

In Figure 17(a), the failure developed on the net tension plane in $[(0^\circ/90^\circ)]_{4s}$ joints is shown. Fiber breakage, fiber/matrix debonding, matrix cracks, and delamination are major failures. In Figure 17(b), as a result of weak interface strength, fiber/matrix debonding and fiber protrusion are seen.

Failure formation in pin connected continuous fiber-reinforced polymer composites is given in Figure 18. As seen in the figure, according to the stacking sequence of the laminates, formation of different failures in the connection area is in question. Failure mechanisms described here schematically, closely affect the load-bearing performance of pin connections. Also, load-bearing performance differs by the plane on which failure develops. The difference here is explained with different failure mechanisms effective on different planes.

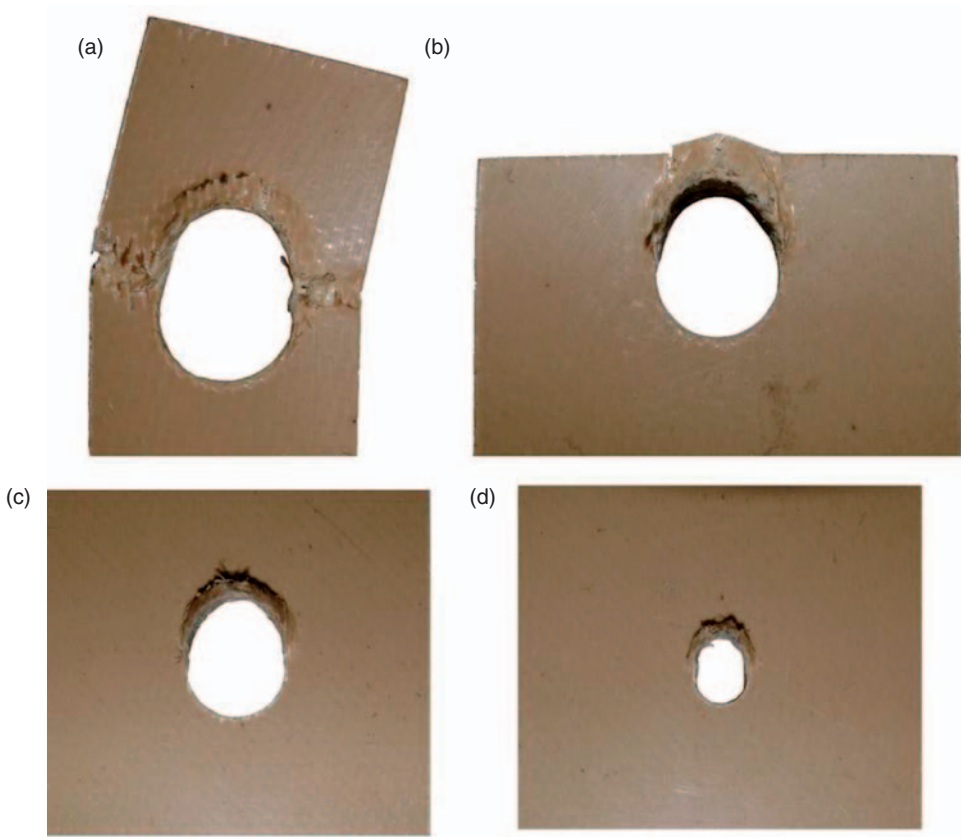

Figure 15. *Photographs of failed pin-loaded $[(0^\circ/90^\circ)/(+/-45^\circ)]_{2s}$ joints: (a) bearing-net tension failure (E/D = 2, W/D = 2, D = 10 mm), (b) shear out failure (E/D = 1, W/D = 4, D = 10 mm), (c) bearing failure (E/D = 2, W/D = 4, D = 10 mm), (d) bearing failure (E/D = 4, W/D = 8, D = 5 mm).*

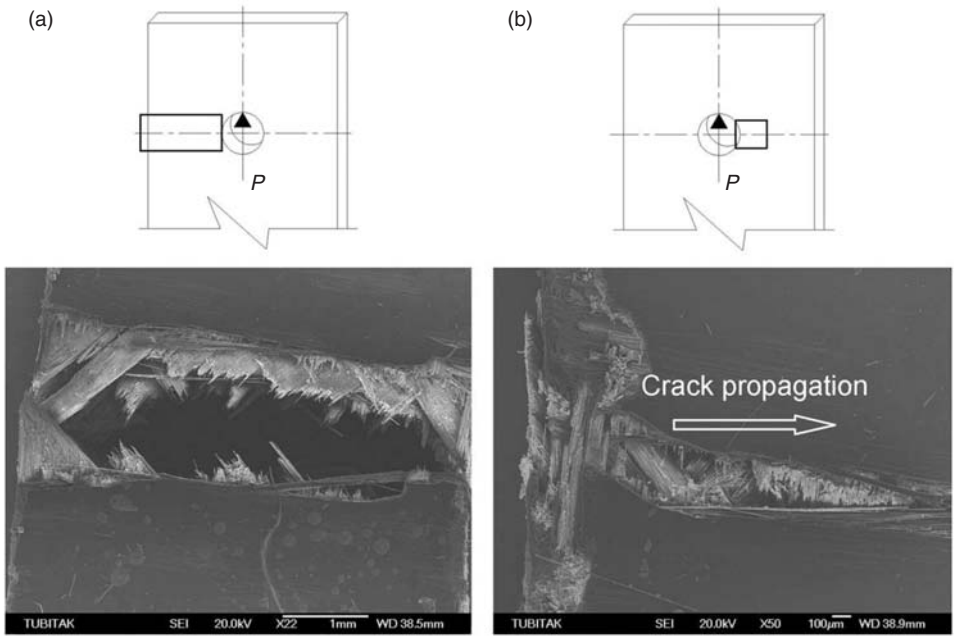

Figure 16. *SEM images of failed* $[(0^\circ/90^\circ)/(+/-45^\circ)]_{2s}$ *lay-up: (a) net tension failure, (b) crack propagation and fiber fracture because of the upward movement of the pin.*

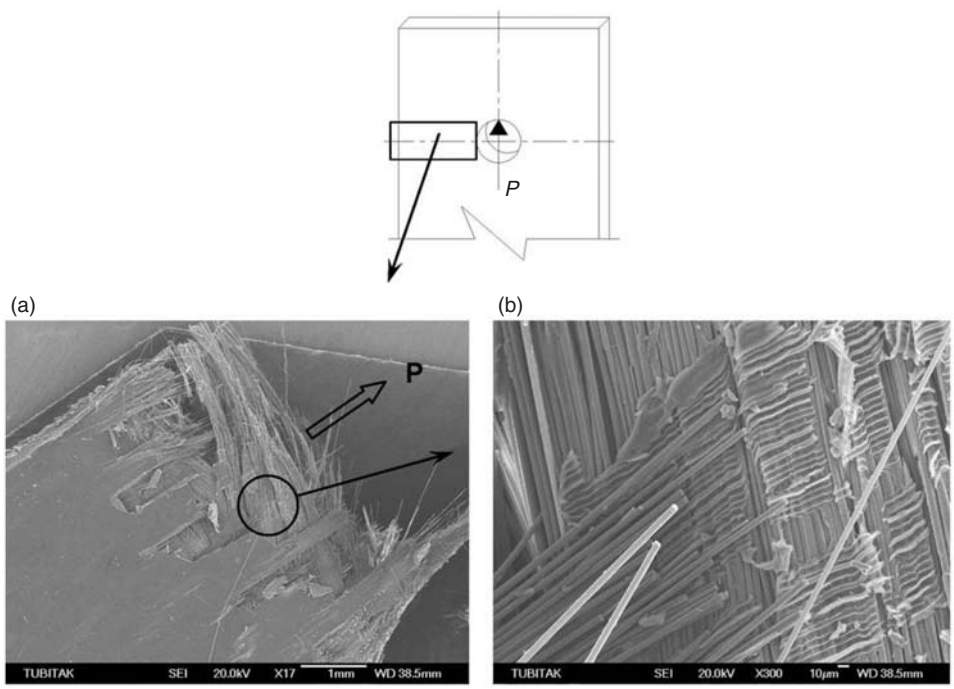

Figure 17. *SEM images of failed pin-loaded* $[(0^\circ/90^\circ)]_{4s}$ *joints: (a) failure at the net tension plane, (b) fiber/matrix debonding and fiber breakage.*

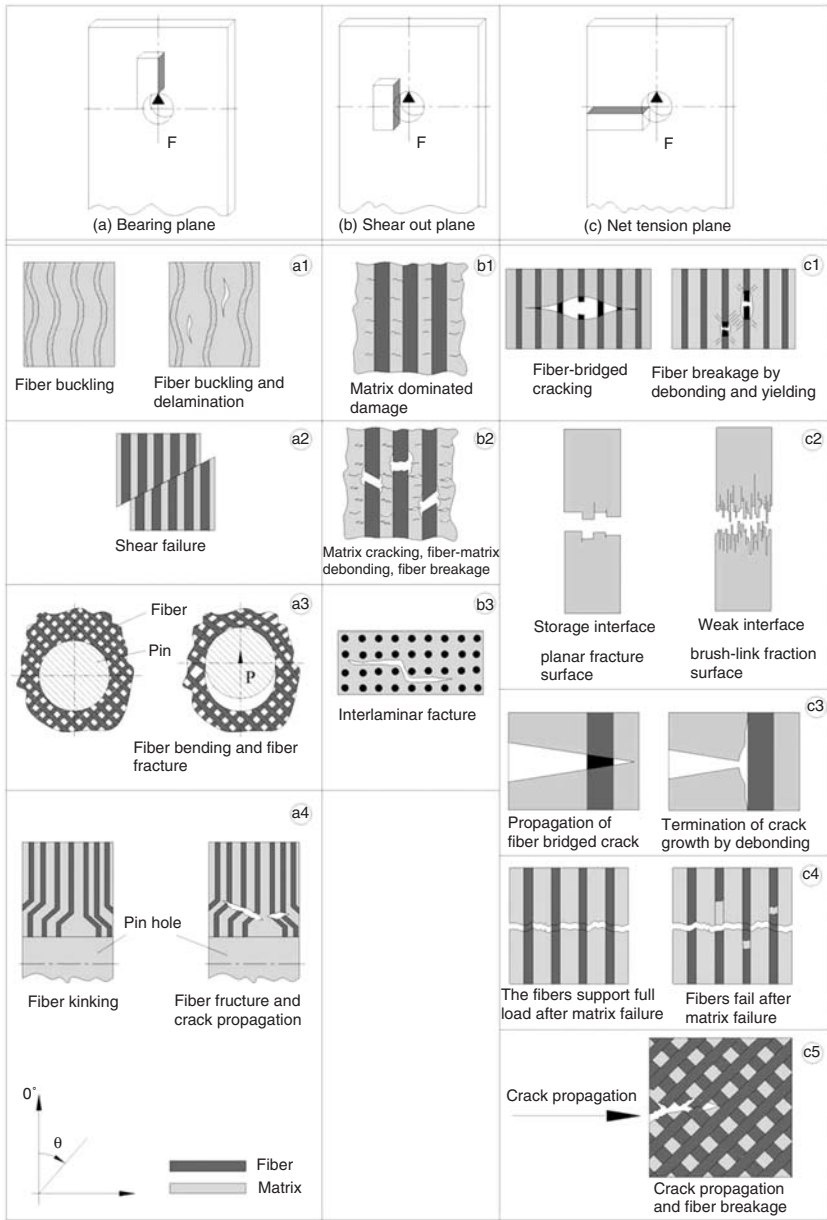

Figure 18. *Schematic illustration of failure mechanisms in pin-loaded joints.*

CONCLUSIONS

In this study, pin joints of multilayered glass fiber-reinforced PPS matrix composites with $[(0^\circ/90^\circ)]_{4s}$ and $[(0^\circ/90^\circ)/(+/-45^\circ)]_{2s}$ stacking sequence were analyzed. The design parameters that were analyzed are listed as: stacking sequence, E/D, W/D ratios, and pin diameter D. It was concluded that the connection behaviors are closely related with geometric parameters. Critical E distance was experimentally obtained and it was proved that

this distance is related with sample width W. After the tests, the results obtained were written below:

(1) The increase in E/D ratio increased the bearing strength. But E/D ratio greater than 4 did not cause an important impact on the connection's load-bearing performance. Thus, the critical E/D ratio is 4.
(2) Ultimate bearing failure loads of the composite plaque increased by increasing the geometric parameters i.e., when the edge distance to diameter E/D increased, but did not change substantially with W/D ratio.
(3) At same E/D ratios, when $D = 10$ mm, in composites having $[(0^\circ/90^\circ)/(+/-45^\circ)]_{2s}$ lay-up, bearing strength is higher with respect to $[(0^\circ/90^\circ)]_{4s}$ lay-up.
(4) In the condition of same E/D ratio and $D = 5$ mm, connections of laminates with $[(0^\circ/90^\circ)]_{4s}$ stacking sequence have higher strength than the $[(0^\circ/90^\circ)/(+/-45^\circ)]_{2s}$ lay-up.
(5) In $[(0^\circ/90^\circ)/(+/-45^\circ)]_{2s}$ joints, when $D = 5$ mm, the increase in W/D ratio, causes an increase also in the ultimate bearing failure load. This situation is acceptable for the given stacking sequence and geometric parameters.

REFERENCES

1. Caprino, G., Giorleo, L., Nele, L. and Squillace, A. (2002). Pin-bearing Strength of Glass Mat Reinforced Plastics, *Composites A*, **33**: 779.
2. Okutan, B. (2002). The Effects of Geometric Parameters on the Failure Strength for Pinloaded Multi-directional Fibre-glass Reinforced Epoxy Laminate, *Composites B*, **33**: 567.
3. Aktas, A. and Uzun, I. (2008). Sea Water Effect on Pinned-joint Glass Fibre Composite Materials, *Compos. Struct.*, **85**: 59.
4. Frizzell, R.M., McCarthy, C.T. and McCarthy, M.A. (2008). A Comparative Study of the Pin-bearing Responses of Two Glass-based Fibre Metal Laminates, *Compos. Sci. Technol.*, **68**: 3314.
5. Atas, C. (2009). Bearing Strength of Pinned Joints in Woven Fabric Composites with Small Weaving Angles, *Compos. Struct.*, **88**: 40.
6. Icten, B.M., Okutan, B. and Karakuzu, R. (2003). Failure Strength of Woven Glass Fibre-Epoxy Composites Pinned Joints, *J. Compos. Mater.*, **37**: 1337.
7. Karakuzu, R., Çalışkan, C.R., Aktas, M. and İcten, B.M. (2008). Failure Behavior of Laminated Composite Plates with Two Serial Pin-loaded Holes, *Compos. Struct.*, **82**: 225.
8. Ahn, H.S., Kweon, J.H. and Choi, J.H. (2005). Failure of Unidirectional-woven Composite Laminated Pin-loaded Joints, *J. Reinf. Plast. Compos.*, **24**: 735.
9. Yilmaz, T. and Sinmazcelik, T. (2007). Investigation of Load-bearing Performances of Pin Connected Carbon/Polyphenylene Sulphide Composites Under Static Loading Conditions, *Mater. Des.*, **28**: 520.
10. Okutan, B. and Karakuzu, R. (2002). The Failure Strength for Pin-loaded Multi-directional Fibre-Glass Reinforced Epoxy Laminate, *J. Compos. Mater.*, **36**: 2695.
11. Karakuzu, R., Taylak, N., İcten, B.M. and Aktas, M. (2008). Effects of Geometric Parameters on Failure Behavior in Laminated Composite Plates with two Parallel Pin-loaded Holes, *Compos. Struct.*, **85**: 1.
12. Quinn, W.J. and Matthews, F.L. (1977). The Effect of Stacking Sequence on the Pin-bearing Strength in Glass Fibre Reinforced Plastic, *J. Compos. Mater.*, **11**: 139.
13. Wu, T.J. and Hahn, H.T. (1998). The Bearing Strength of E-Glass/Vinyl-Ester Composites Fabricated by VARTM, *Compos. Sci. Technol.*, **58**: 1519.
14. Scalea, F.L., Cloud, G.L. and Cappello, F. (1998). A Study on the Effects of Clearance and Interference Fits in a Pin-loaded Cross-ply FGRP Laminate, *J. Compos. Mater.*, **32**: 783.

15. Wang, H.S., Hung, C.L. and Chang, F.K. (1996). Bearing Failure of Bolted Composite Joints. Part I: Experimental Characterization, *J. Compos. Mater.*, **30**: 1284.
16. Thoppul, S.D., Finegan, J. and Gibson, R.F. (2009). Mechanics of Mechanically Fastened Joints in Polymer–Matrix Composite Structures – A Review, *Compos. Sci. Technol.*, **69**: 301.
17. Ireman, T., Nyman, T. and Hellbom, K. (1982). On Design Methods for Bolted Joints in Composite Aircraft Structures, *Compos. Struct.*, **25**: 567.
18. Choi, J. and Chun, Y. (2003). Failure Load Prediction of Mechanically Fastened Composite Joints, *J. Compos. Mater.*, **37**: 2163.
19. ASTM D 953-D, Standard Test Method for Bearing Strength of Plastics, ASTM Designation, 342.